ʻIMAKA: Imaging from MAuna KeA optical design

Clinton Evans*[a], Hua Lin[a], Ashley McColgan[a], Neil Rowlands[a], Derrick Salmon[b]
[a]COMDEV International Ltd., Ottawa, ON, K2K 3J1, Canada;
[b]CFHT Corporation, 65-1238 Mamalahoa Hwy, Kamuela, Hawaii 96743, USA

ABSTRACT

The ʻIMAKA (Imaging from MAuna KeA) instrument is a wide field visible light imager incorporating Ground Layer Adaptive Optics (GLAO) to take maximum advantage of the excellent seeing available at the Canada-France-Hawaii Telescope (CFHT). It requires better than 0.3″ image quality simultaneously over a total field of view of approximately one square degree (~3 x 10^{-4} sr). This requirement along with other criterions and constraints raises a challenge for optical design. The advent of orthogonal transfer (OT) CCDs allows the tip-tilt portion of the atmospheric correction to be performed at the science detector itself. ʻIMAKA will take full advantage of the large array mosaics of OTCCDs. Since the size of the adaptive mirror would drive the cost and hence implementation of the overall ʻIMAKA instrument, a review of possible optical design configurations which minimize the size (diameter) of the deformable mirror is undertaken. A promising design was obtained and developed in more detail. This all reflective system is described along with its predicted optical performance. An opto-mechanical design concept was developed around this nominal optical design which takes into account various constraints due to its required location on the top end of the Canada France Hawaii Telescope. The design concept is feasible and meets the optical performance requirements.

Keywords: optical design, wide-field imaging, TMA, deformable mirror

1. INTRODUCTION

1.1 Background

Canada-France-Hawaii Telescope (CFHT) has provided spectacular images of the heavens and produced significant discoveries in astrophysics. The ʻIMAKA (Imaging from MAuna KeA) instrument, the next generation of CFHT instrumentation, is a wide field visible light imager incorporating Ground Layer Adaptive Optics (GLAO) to take maximum advantage of the excellent seeing available at the CFHT. The primary design goal is to obtain better than 0.3″ image quality simultaneously over a total field of view of approximately one square degree (~3 x 10^{-4} sr). Modeling has shown that this can be accomplished via use of GLAO which also incorporates tip-tilt correction [1] to remove atmospheric turbulence and turbulence arising around or within the optical system enclosure. The advent of orthogonal transfer (OT) CCDs makes the tip-tilt correction function possible at the science detector itself. Large array mosaics of OTCCDs developed and deployed in other instrumentation such as the GigaPixel Camera 1 for the Panoramic Survey Telescope & Rapid Response System (Pan-STARRS) [2] and the One Degree Imager (ODI) on the WIYN telescope [3]. ʻIMAKA will take full advantage of the technology.

This paper is arranged as follows. First a discussion of the design requirements and constraints, followed by a review of possible optical layouts that arose in the initial feasibility studies, is presented in section 1. A more detailed optical design for a promising optical layout is developed in section 2, along with some predictions of performance. Section 3 develops the mechanical layout for the proposed optical system. Finally, in section 4, a summary of the study is presented.

Clinton.Evans@comdev.ca

1.2 Optical Design Requirements and Design Constrains

The primary design goal is to obtain better than 0.3″ image quality simultaneously over a total field of view of approximately one square degree (~3 x 10^{-4} sr). A complete listing of the optical requirements is shown in the middle column of Table 2 in section 2 as comparison with design results. The design is constrained by both the current CFHT primary mirror prescription and by the current CFHT mechanical layout. Figure 1 shows the top end handling fixture and provides an indication of the operations required to change out the top end of the CFHT. This includes the equipment used to manipulate the top end. This is currently done with instrumentation such as MegaCam [4]. In terms of 'IMAKA accommodation the following three regions within the CFHT were considered, refer to Figure 2:

A) above the top ring structure of the telescope
B) within the "Caisson central" in line with the rotation axis of the telescope body within the mount
C) at the Cassegrain focus of the telescope (with freedom to choose secondary mirror parameters).

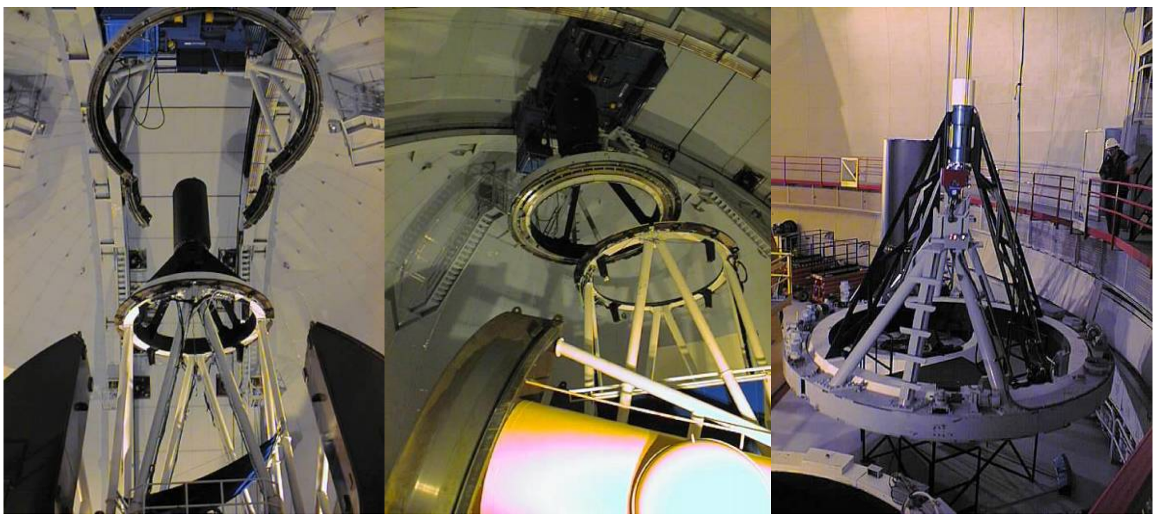

Figure 1 CFHT Top End Replacement Operations

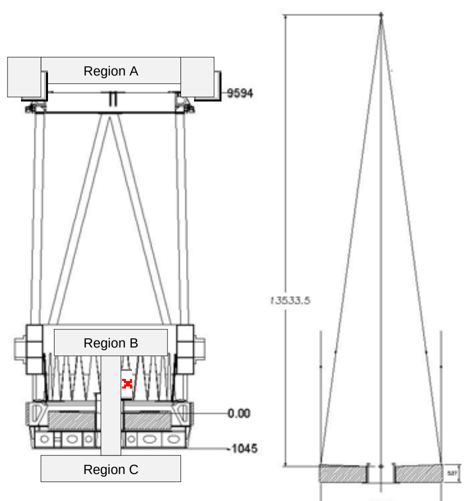

Figure 2 CFHT Layout showing regions considered / available for 'IMAKA optics

1.3 Optical Layout Examples

The following factors influenced the eventual selection of the optical layout:

- maintenance access for the detector focal plane
- maintenance access for the deformable mirror
- minimizing the obscuration

In case A and B the bulk of the 'IMAKA optics located in the path would have to be arranged to primarily fall within the central obscuration. Although it would be possible to distribute the 'IMAKA optics to within two or more of these regions, including through the primary mirror between regions B and C, these regions are sufficiently far apart, that such a layout would likely make the optical elements prohibitively large. Note that Region A is considered to extend beyond the outer diameter of the top ring at least above the top ring itself. This is because this region can has clearance above the horseshoe mount when the telescope is oriented to high declinations. Ideally any instrument / optics intended for mounting on the top ring of CFHT should be compatible with the infrastructure that is available.

'IMAKA GLAO correction requirements implies a re-imaging of the telescope pupil near the location of the primary mirror aperture. This can be accomplished onto a relatively small internal aperture, where the deformable mirror (DM) is to be located, if a relatively small distance from prime focus is maintained. As the distance between prime focus and the internal pupil grows, it becomes very difficult to re-image the pupil at the correct size. For this reason, options involving Regions B and C were rapidly ruled out. A number of possibilities for optical layouts confined to Region A (top ring mounted) were considered. These options build on the Region A solutions incorporating an adaptive secondary mirror as shown in Figure 3 (a) and Figure 3 (b).

Adaptive secondary mirrors have been implemented at other observatories notably the MMT and the LBT [5]. However such a mirror for CFHT would require an extension of this technology to a somewhat larger diameter mirror and would also require monetary expenditures which would dominate the cost of implementing 'IMAKA. Since such a device would drive the cost and hence implementation of the overall 'IMAKA instrument, alternatives to a large diameter deformable mirror are sought. Figure 3 (b) represents an initial attempt to reduce the size of the DM by making use of on-axis relay optics. However, as is apparent in the figure the design incurs a large central obscuration when all the optics is kept centered. The obscuration can be reduced by making use of a three mirror off-axis relay, with one of the relay mirrors being the deformable mirror, as per the example shown in Figure 3 (c). However the obscuration is still fairly large, and now is asymmetric as well.

Thus we primarily explored alternatives that placed some or a majority of the instrument optics outside of the main aperture. Figure 3 (d) represents one possibility which has a small DM in the central obscuration but places the rest of the optics (including a science camera – not shown) outside the main aperture. This type of system could also make use of refractive optics, such as shown in Figure 3 (e), where a combination of a refractive composite field lens and collimator is used to relay the pupil external to the aperture. The issue with this type of system is obtaining the required low angle of incidence and reflection at the DM (which would be the next surface in the figure, but is not shown). One possible solution to this issue is to make use of total internal reflection in a prism like arrangement shown in Figure 3 (f). The beam leading to the science camera would exit from the left of the prism shown in the figure. However procuring such large prisms in high index material with the requisite high optical quality could prove problematic.

Since the concepts making use of a simple fold mirror, see Figure 3 (d), to relay the beam to the side of the aperture showed promise and the refractive designs required large difficult to procure elements, all reflective designs were considered instead. In the following sections, we will present a promising optical and opto-mechanical design concept based on the reflective system.

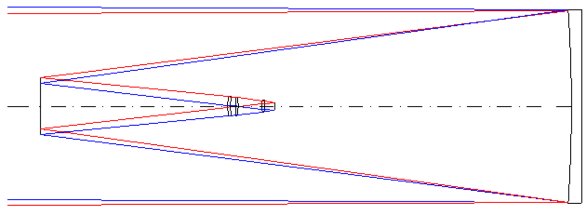

(a) using adaptive secondary

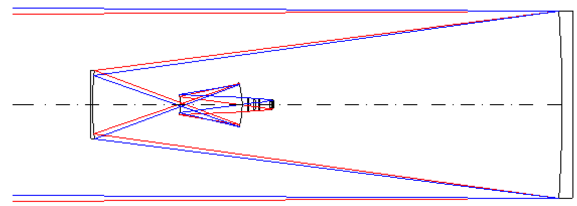

(b) with adaptive tertiary mirror

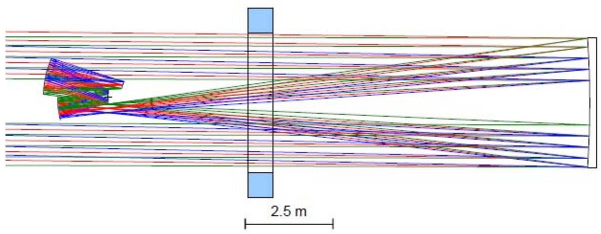

(c) with relay embedded in central obscuration

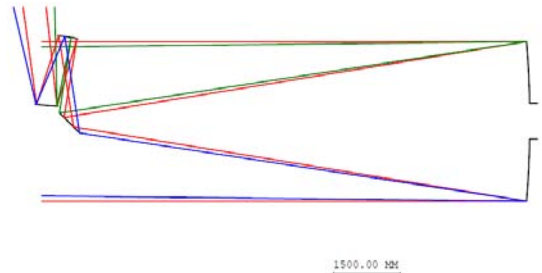

(d) with DM in central obscuration

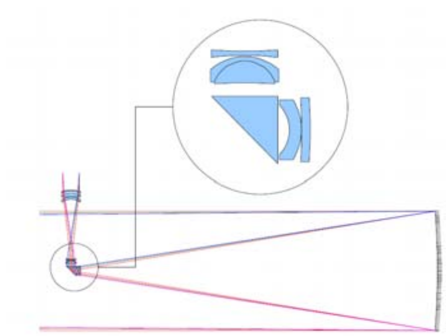

(e) with refractive relay

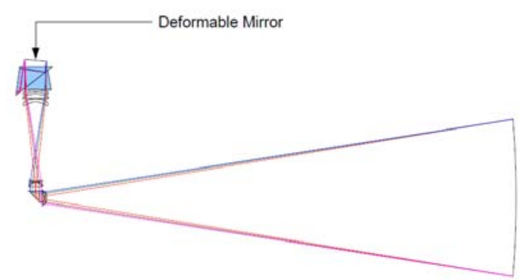

(f) using total internal reflection as a packaging aid

Figure 3 ‘IMAKA Optical Layout with Different Concepts

2. SELECTED OPTICAL DESIGN AND PERFORMANCE

2.1 Optical Layout

We further optimize the reflective system based on Figure 3 (d). Shifting the field slightly off-axis on the CFHT primary mirror was found to be quite effective in optimizing the subsequent three mirror design, which is by necessity off-axis. Such a system has a number of advantages especially if the pupil image can be arranged to fall on one of the three mirrors and the radius of curvature of this mirror can be large, allowing this mirror to become the DM. The main possible drawback is that such a system naturally accommodates a rectangular field of view better than a square or circular field of view. Since ‘IMAKA is primarily concerned with sky coverage (total solid angle) then it is possible that a rectangular field of view which meets the ~1 square degree requirement would be acceptable scientifically. Another concern is that due to the large field of view the mirrors in such a relay system become quite large. This can be mitigated by splitting the field of view between two separate relay systems. The optics are arranged to be closer to the mounting ring and the fold mirror is adjusted to make the overall packaging smaller. Figure 4 shows a two dimensional layout of the IMAKA telescope optical system. A three dimensional view is shown in Figure 5 and Figure 6. The prescription data for each of the optical elements of one channel, along with their CODE V mnemonics, are shown in Table 1.

The two-channel approach has a number of benefits:

- The optical design is feasible.
  - A single-channel reflective solution is very difficult and may not be feasible.
  - Minimizes the DM aperture (~250 mm in this design)
- The center of gravity is close to the axis of the telescope structure.
- Makes the DM and focal plane relatively accessible adjacent to the top ring
- Cost:
  - A single-channel solution requires very large mirrors.
  - Two identical, smaller mirrors are generally more cost effective than one large mirror.
- Redundancy
  - If only one channel is operational, observation is still possible.

For purposes of optimization, the aperture stop is placed at the CFHT main mirror. A pair of fold mirrors tilted ±40˚ with respect to the telescope axis split the imaging ray bundle into the two channels. Each channel has a three-mirror relay system to produce an image on the detector. The nominal focal plane is convex with a radius of curvature of 1.6 m. Because of the large field of view the focal plane will be populated by a fairly large number of individual detector arrays which can be arranged in piston and tilt to best approximate the convex focal plane. The resulting correction at the detector is very good and provides useful margin for manufacturing and environmental budgets. The secondary mirror of the relay, which is deformable and located at the intermediate image of the aperture stop, provides a means of correcting atmosphere-induced wavefront errors. Tip-tilt of the fold mirrors provides alignment adjustment. A detector piston movement could provide the focus adjustment. This adjustment may be motorized for adjustment during observation. Other alternatives for focus adjustment are discussed in section 2.3.

Table 1 Component Prescriptions

Surface Name	**Surface Parameter**			**Aperture**
	Type	**Radius**	**Conic constant**	
Ring				Φ 4000
Main Mirror	Asphere	-27067.000	-1	Φ 3620
Fold M1		Infinity		516×590
Primary	Asphere	-1817.8705	-4.7662	650×500
Adaptive	Sphere	-1626.0205		Φ 260
Tertiary	Sphere	-2917.0385		910×640
Fold M2		Infinity		660×680
IMG		1633.6462		360×150

Unit: mm

2.2 Field of View Layout

The image size on the detector is 363×143 mm^2 corresponding to a full field of view of 1° × 0.3927°, i.e., 0.1 arcsec per 10 µm pixel. The two 'IMAKA channels have fields of view which are separated on the sky by about 2° as shown in Figure 7. Because of the arrangement of the channels, when pointing along the meridian, this separation is along the declination direction. For large area sky surveys, dithering over the course of many hours will help to "fill-in" the surveyed area.

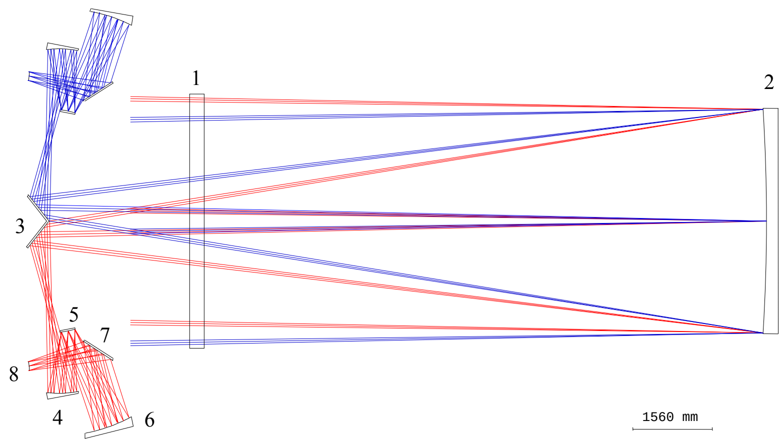

1: Top ring, 2: Primary 3: Fold 1, 4: Primary, 5: Deformable, 6: Tertiary, 7: Fold 2, 8: Detector

Figure 4 ' IMAKA & CFHT optical layout (Three Mirror Relay)

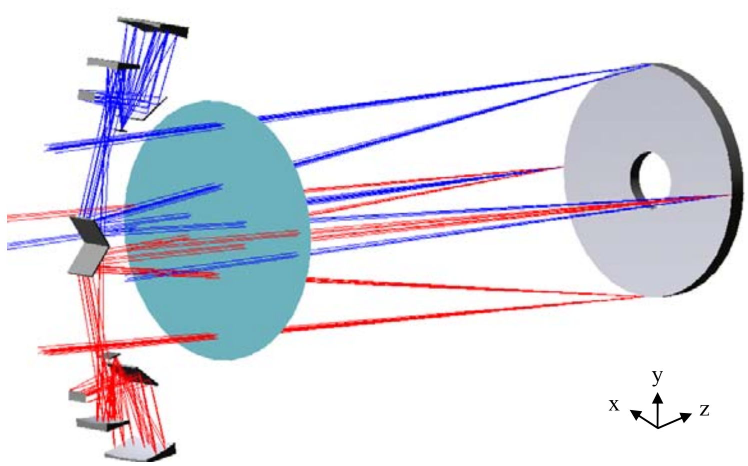

Figure 5 Three-dimensional view of the 'IMAKA optical concept

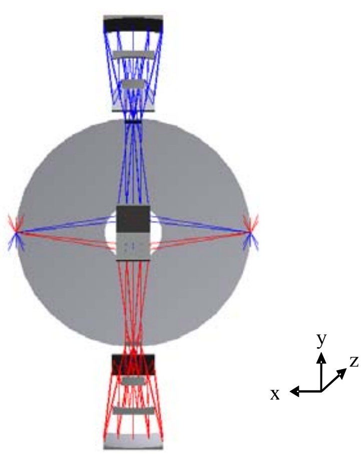

Figure 6 Front view of 'IMAKA optical concept

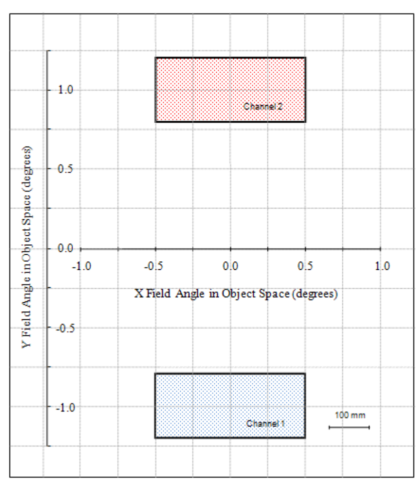

Figure 7 Projection of 'IMAKA field of view on the sky

2.3 Optical Performances

2.3.1 Ray Aberrations

The ray aberrations are shown in Figure 8, again for 587.6 nm wavelength. The main aberrations are astigmatism and Petzval blur.

2.3.2 Spot Diagrams

Figure 9 shows the CODE V spot diagram plot of different fields.

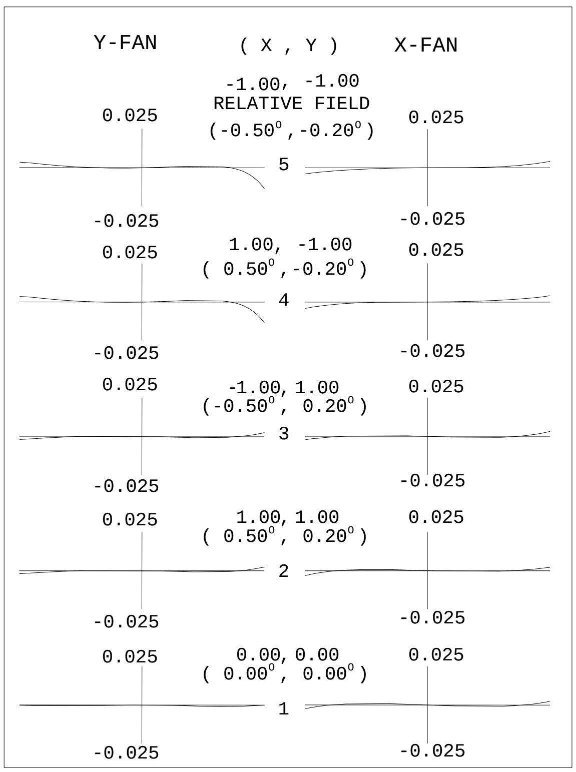

Figure 8 Ray aberration

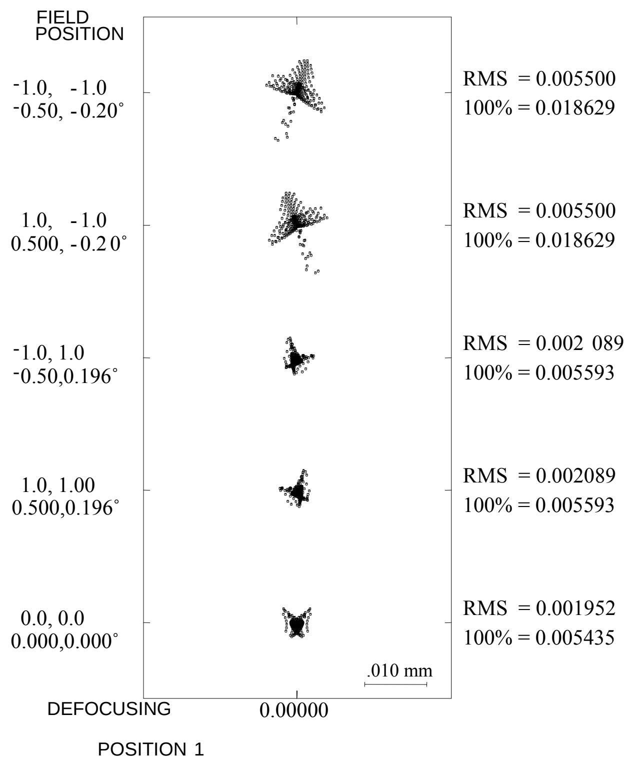

Figure 9 Spot diagram

2.3.3 Imaging RMS Wavefront Error

Figure 10 shows the RMS wavefront error of the telescope and 'IMAKA design prescription for channel 1. The field comprises 363×143 mm^2 regions of the image surface. Field centre is located in the center of the focal plate. The diameter of each circle represents the local RMS error. The scale indicates a diameter equivalent to 1 λ RMS. The maximum RMS WFE is about 123 nm in the neighborhood of (0.0˚, 0.2˚). The region where the design aberrations approach the requirement limit is shown as the trapezoidal region.

The optical design has high image quality over a considerably larger FOV than is required, as shown by the larger scale wavefront error map in Figure 11. Within the area of the rectangular shape from (-1˚, -0.37˚) to (1˚, 0.20˚), marked by dash line in the figure, the image is also acceptable. The apertures of the components would have to be enlarged considerably to take complete advantage of this, for example, the aperture of the deformable mirror required to accommodate a FOV this large would be 400×260 mm, but this does provide an indication of potential performance.

This extended field of view also indicates regions which are potentially accessible for wavefront sensing, especially if a small amount of vignetting can be tolerated by these sensors.

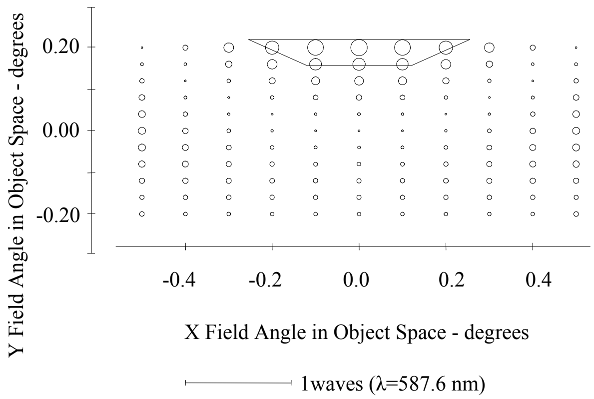

Figure 10 RMS wavefront error

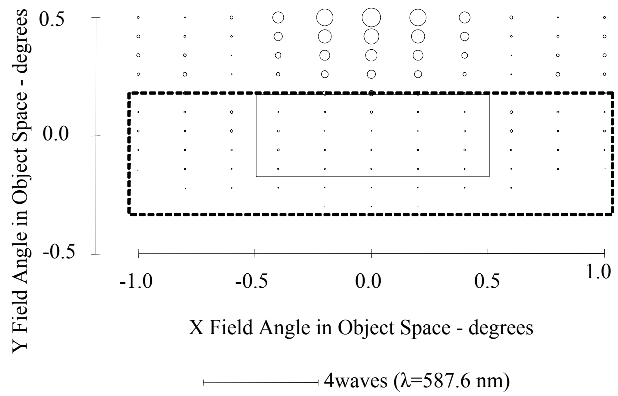

Figure 11 Wavefront: theoretical extended FOV performance

2.3.4 Point Spread Function (PSF) and Encircled Energy

The PSF and encircled energy plots are shown in Figure 12 and Figure 13, respectively. 80% encircled energy diameter is about 0.01 mm, i.e., 0.10 arcsec corresponding to the field on the sky. The worst case is at the edge field of (0.0˚, -0.2˚) which is 0.02 mm (equivalent to 0.20 arcsec) 80% encircled energy. Refer to the Figure 10, the RMS wavefront error map, the area where encircled energy diameter is larger than 0.015 mm (within the trapezoid) is 5% of the total field. More than 90% FOV 80% encircled energy diameter is less than 0.15 arcsec.

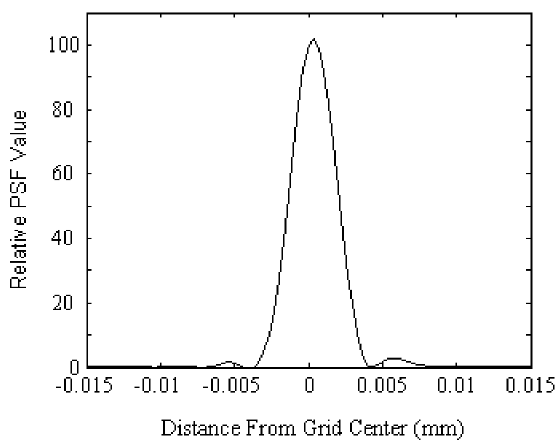

Figure 12 PSF plot

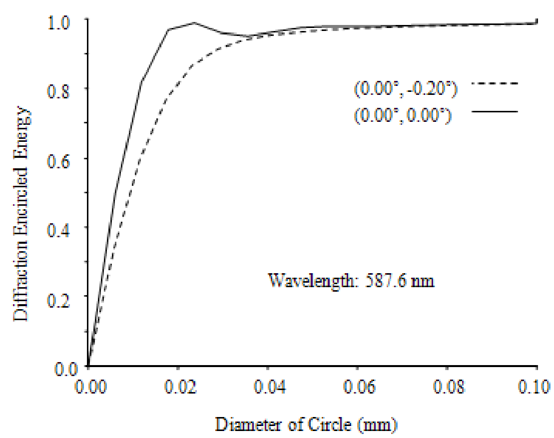

Figure 13 Encircled energy plot

2.3.5 Other Characteristics

The distortion is less than 0.6% with respect to paraxial. The footprints are a good fit on the mirrors apertures with margin. The pupil aberrations are quite small with the worst case approximately 5.1% of the pupil image diameter on the deformable mirror.

2.4 Focus Considerations

2.4.1 Focus Adjustment

The distance between the fold mirror M1 and the CFHT primary mirror will vary due to temperature change. Given the expected temperature changes during an observing run the physical separation is likely to change on the order of 0.5 mm. If M1 moves 0.5 mm closer to the main mirror, the average WFE degrades to 2 λ from 0.07 λ. Thus clearly focus compensation is required. There are several ways to compensate the misalignment:

- Move detector 1.18 mm away from the fold mirror M2. The image quality would then recover to be close to the ideal. 80% encircled energy diameter is 0.01 mm and average WFE is 0.08 λ.
- Adjust the fold mirror M2 1.18 mm away from the tertiary mirror. This has the similar result as adjusting detector. This option is superior to moving detector and is our preferred choice.
- Move fold mirror M1 back 0.25 mm. However, the image quality degrades. The 80% encircled energy is 0.03 mm. The average WFE degrades from 0.07 λ to 0.5 λ.

This we cannot compensate for focus change by displacing M1 alone other compensation is required – and the preferred approach at this time appears to be a repositioning of the fold mirror (M2) as the on-instrument focus adjustment.

2.4.2 Defocus WFE at Focal Plane

As mentioned earlier, there is an intrinsic mis-match between a flat detector surface and the actual curved image plane formed by the optics. Since the focal plane detectors must be tiled mosaics of smaller detector arrays due to the intrinsic limits of the technology, the science detector will be constructed of a mosaic of OTCCDs with a format similar to those used for the PanSTARRS focal plane, which made use of 60 4k×4k OTCCDs from MIT Lincoln Laboratories. The focal plane required for one channel of the 'IMAKA mosaic will be about 30% smaller than this PanSTARRS focal plane, requiring 10×4 4k×4k 10 μm pixel OTCCDs, though covering 1 square degree of sky at a sampling of 0.1″/pixel with the two 'IMAKA channels will require a total of 80 4k×4k OTCCDs. The form factor of the Pan-STARRS focal plane was used to estimate the required form factor for the 'IMAKA focal plane in the opto-mechanical packaging concept. Note that the Pan-STARRS design was constrained by constraints not applicable to 'IMAKA, such as a relatively "flat" arrangement. For 'IMAKA the focal plane electronics can be placed behind the detector arrays.

For a 4096×4096 pixels (10 μm/pixel) detector cell, the maximum offset is 0.128 mm from the designed curve image plate if the centers of the detectors are placed at the nominal image surface. The average WFE degrades to 0.023 λ and the 80% encircled energy diameter is 0.025 mm due to the mismatching between the detector flat surface and designed image surface. If the detectors are arranged in the way that their centers are 0.064 mm in front of the nominal curve surface, the average WFE is about 0.01 λ and 80 % encircled energy diameter is 0.014 mm, which meets the requirement. Thus it is feasible to compensate for the curved focal plane in this manner. An array composed of smaller detector formats would certainly be better for matching the nominal image surface. For example, the effect of a flat surface of a detector of 2048×2048 pixels (10 μm/pixel) is negligible. Since smaller detector means more work for the focus butting and registration, a detector size intermediate between 20 mm and 40 mm on a side may be desirable.

2.5 Adaptive Optics System

2.5.1 Deformable Mirror

The deformable mirror technology most suitable for 'IMAKA is the "Piezo-Array" technology, which has been developed by CILAS (Orleans, France). The size of these DM's (for example 188 mm diameter for the system delivered to ESO) compares favorably with the size required by the 'IMAKA optical concept described in this document [6].

2.5.2 Wavefront Sensing System

Wavefront sensors for adaptive optics systems have been deployed and are in use at a number of observatories around the world. These systems generally have a very small field of view and in the case of WFS for natural guide stars they have actuated pickoff optics small mirrors reorienting the image to several small detectors, typically CCDs, so that appropriate guide stars can be found within the overall science imaging field of view. The auxiliary optics for these wavefront sensors can be based on binary optics or Shack-Hartmann lenslets ([7], [8]). The distortions induced by the atmosphere is then interpreted by processing multiple defocused (or focused) images using retrieval algorithms. Output signals are generated to control the deformable mirror and to bring the measured wavefront into closer conformance with the ideal.

If the required patrol field of view of a WFS is very large then the opto-mechanical arrangement can become complex. The WFS requirements for ‘IMAKA are challenging since as many as half a dozen natural guide stars may be required to be accessible to the WFS across the full ‘IMAKA field of view [9]. Figure 11 shows that the optics design does support a large FOV for the WFS to patrol adjacent to the science field of view.

2.6 Optical Design Verification Matrix

The resultant optical system is summarized in Table 2 comparing with the requirements.

Table 2 Comparisons between requirements and preliminary design results

Parameter			Requirements	Design Results	Notes
1	Wavelength Range		150 nm wide bandpass centered from 470 nm through 900 nm	Reference: 587.6 nm	The optical design is a reflect system. It works for any band within the requirement.
2	Field of View		1˚ 1 square degree (~3 x 10^{-4} steradians) Does not have to be contiguous nor is a particular shape required	1˚×0.3927° for one channel	The total scanned sky area of the two channels is equivalent to the area of 1˚ circular field.
3	Image Scale		0.1 arcsec per 10 µm pixel	0.1 arcsec FOV per 10 µm	
4	Main Mirror Diameter		3592 mm	3592 mm	
6	Focus Length (F number)		20.63 m (F#/5.74)	20.83 m (F#/5.80)	
7	Image Quality		0.15 arcsec 80% encircled energy across the central 90% of a 1˚ diameter field	80% encircled energy diameter is 7.78 µm, i.e., 0.08 arcsec	The optical design is diffraction-limited and has useful margin over the requirement.
8	Science Camera	Location	Above the top ring and the telescope trusses or below the Cassegrain environment a)Above top ring (A) b)Caisson Centrale (B) c)Near Cassegrain focus (C)	Above the top ring	
9	Deformable Mirror	Diameter	< 500 mm	254 mm (Clear aperture)	
		Conjugate Location	within 20 m below the main mirror to 50 m above the main mirror.	7.8 m below the main mirror	
		Incident Angle	< 30˚	< 24˚	

3. OPTO-MECHANICAL PACKAGING

3.1 Description

The opto-mechanical packaging concept for the 'IMAKA design is shown in Figure 144, 15, and 16 along with the ray trace overlay from the optical design. Note that some obscured rays are shown. The expected obscuration of the aperture is discussed later in this paper.

The main 'IMAKA structural support, which mounts to the CFHT top ring is shown in orange and is designed to be compatible with the current top ring handling fixtures and infrastructure (as shown in Figure 14). Since the structure of the CFHT telescope is assumed to be made from mild steel, then ideally the 'IMAKA support structure (the extensive structure shown in orange) should also be manufactured using the same or similar steel to minimize distortions over the operating temperature variations. Due to the protrusion of the 'IMAKA optics outside the top ring, the existing handling equipment may dictate that the 'IMAKA optical paths lie on the north-south declination axis (see the left panel in Figure 1).

As shown in Figure 15, the main optical structure holding the powered mirrors, the deformable mirror and the fold mirror is shown in light blue, the focal plane array is mounted to this structure (as shown in yellow), as is the filter wheel (red). Space is reserved for the wavefront sensing optics and mechanisms just in front of the focal plane array (orange box). Baffles are not shown, but one possible baffle arrangement would be to place an aperture at the prime focus of the primary mirror (shown at left top of the bottom image in Figure 15). Although the 'IMAKA concept selected does not show much internal baffling, the ability to baffle at this prime focus field stop and at the deformable mirror (ie. at the internal pupil) should provide robust stray light control.

Each 'IMAKA channel will have an "optical bench" which maintains the tight mechanical tolerances between each of the optical elements. Ideally the optics plus bench would be made from similar materials and thus scale with temperature changes. In addition, it would be advantageous to select a reasonably conductive material such as aluminum or steel that would help to minimize thermal gradients that could cause distortions and misalignment between the optical bench and the critical optical surfaces. While an all metal solution may be attractive in many ways it will be a challenge to produce the optical surfaces required to meet the short wavelength performance required. Nickel plated metal (over aluminum or even steel) is a possible solution since the surface can be post-polished to achieve the required surface figure and roughness for good short wavelength performance and understanding the bimetallic effect between the nickel coating and the base material needs to be considered.

Alternatively to an all metal solution the use of mirrors made of a low CTE material such as Zerodur mounted to an optical bench fabricated from an appropriate steel alloy via a set of flexures made from a low CTE metal such as invar has a lot of heritage. The mix of materials make the instrument less tolerant to bulk temperature changes, but unlike the all metal solution it is also less sensitive to temperature gradients because of the low overall CTE of the materials.

The behavior of the DM surface will not be athermal with respect to the rest of the optics, since it is supported by piezo-electric material and special considerations will need to be taken to how it is mounted to the structure.

3.2 Obscurations

As shown in Figure 16, the mechanical support for the TMA camera and the adaptive control system for the deformable mirror will block some light coming to the telescope. The fold mirrors M1 do not contribute much to the total obscuration since almost all the light that they potentially could block is located in the central unreflective area of the main mirror. The total obscuration is about 4.5% with respect to the effective area of the entrance pupil. The footprint for the center field of the entrance pupil considering mechanical structure is plotted in
Figure **17**. Note that this is the obscuration for one of the channels, the obscuration for the other channel is the same amount but just asymmetric on the opposite side of the aperture. The DM housing from one channel provided most of the obscuration for the other channel.

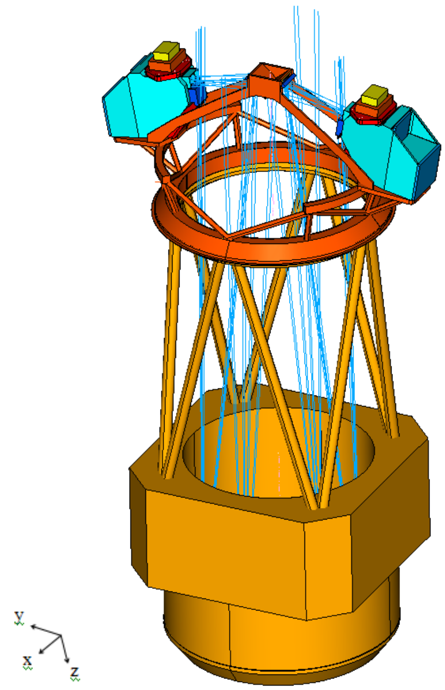

Figure 14 CFHT and ‘IMAKA opto-mechanics with raytrace

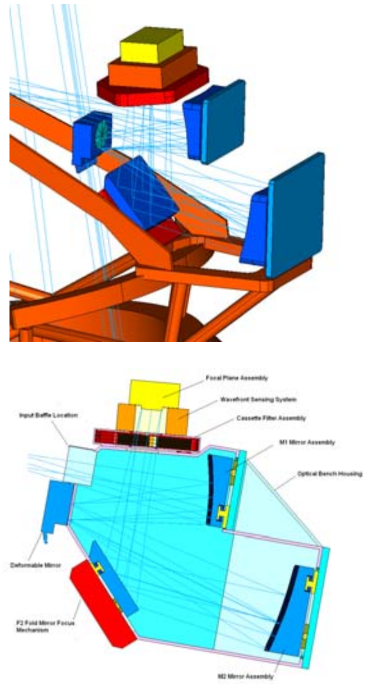

Figure 15 one IMAKA channel optical path & housing

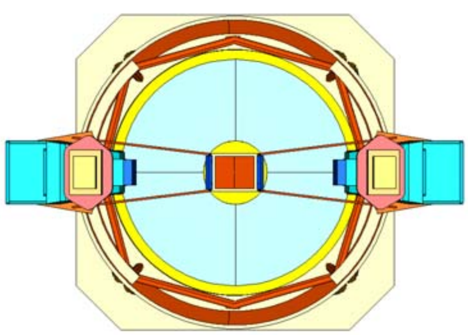

Figure 16 Top view of ‘IMAKA

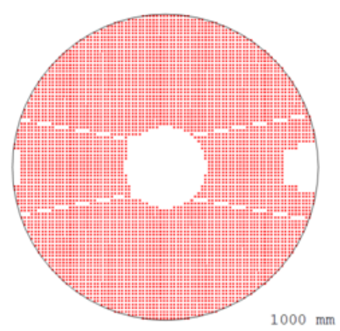

Figure 17 Footprint on entrance pupil considering obscurations (for left channel)

3.3 Envelope

The fit within the observatory is an important consideration to assess the feasibility of the ‘IMAKA concept. The overall dimensions are 7.175 m × 4.96 m × 3.175 m (L×W×H). The length of the layout is driven by the second powered mirror (M2) on the back end of each channel. This extension however is localized and only approximately 0.95m wide. The overall height is driven by the focal plane assembly which is only slightly taller than the central obstruction at 3.175m.

As stated previously, a design constraint considered for the ‘IMAKA concept was the benefit of mounting to the top ring of CFHT with the existing infrastructure that is available (i.e. the Handling Ring). To allow access for the Handling Ring the upper end structure was notched on either side of the ring opposite to the optical channels as shown in.

The overall mass of the `IMAKA instrument based on a steel structure contruction with flexure mounted Zerodur optics was estimated to be approximately 9834 Kg, This compares favorably with MegaCam another CFHT top ring mounted instrument [4], which has an overall top end mass of 8680 kg.

At over 4220 Kg the largest contributor to the mass is coming from the Upper End Assembly which interfaces to the telescope top ring and supports the two `IMAKA channels. If necessary, it would be feasible to optimize the design of this structure and reduce the overall mass of the `IMAKA instrument by 25%. Each `IMAKA optical channel is estimated to be 2294 Kg with approximately half of this mass attributed to the housing. Again through optimization of the housing design this mass could be reduced by 25%. Each of the mirrors in the design was modeled as a monolithic block attached via a set of Invar flexures. Light-weighting of the optical elements would further reduce the overall mass of the instrument if mass becomes a major design driver.

The ‘IMAKA design is balanced with each channel located directly opposite each other. The centre of gravity of the ‘IMAKA concept is located very closely along the optical axis of the telescope and approximately 1.44 m above the top ring interface.

4. CONCLUSION

This paper presents an ‘IMAKA opto-mechanical concept design in order to assess feasibility over the overall ‘IMAKA concept. The ‘IMAKA concept depends on the provision of excellent image quality over a large field of view using a deformable mirror system. Some optical design options has been discussed and an all reflective off axis system has been chosen for study. Two identical channels are applied to cover the required large field of view. It has been demonstrated that the chosen two-channel all reflective off-axis system meets the optical performance requirements and can be packaged and integrated into the CFHT. The ‘IMAKA concept is indeed feasible on CFHT with minimal disruption to the telescope and nominal observatory operations.

ACKNOWLEDGEMENTS

The work was supported by the Canada-France-Hawaii-Telescope Corporation. The authors gratefully acknowledge the ‘IMAKA co-Principal Investigators, Harvey Richer (UBC) and Ray Carlberg (University of Toronto), and CFHT Corporation for the opportunity to participate in the ‘IMAKA study.

REFERENCES

[1] Feasibility Report for ‘IMAKA ‘IMAKA Team, October 1, 2008 http://terapix.iap.fr/IMG/pdf/IMAKA_Feasibility_Report.pdf

[2] Onaka, P., Tonry,J.L., Isani, S., et al. The Pan-STARRS Gigapixel Camera #1 and STARGRASP controller results and performance. Proc. of SPIE Vol. 7014, 70140D (2008)

[3] Harbeck, D.R., Jacoby, G.H., and Muller, G., et al, The WIYN One Degree Imager: An Update. Proc. of SPIE Vol. 7014, 70144Q (2008)

[4] Boulade, O., Charlot, X., Abbon, P., et al. MegaCam: the new Canada-France-Hawaii Telescope wide-field imaging camera, Proc. of SPIE Vol. 4841 (2003)

[5] Riccardi, A.; Xompero, M.; Zanotti, D.; et al. The adaptive secondary mirror for the Large Binocular Telescope: results of acceptance laboratory test, Proceedings of the SPIE, Volume 7015, pp. 701512-701512-9 (2008)

[6] Sinquin, J.-C.; Lurçon, J.-M. and Guillemard, C. Deformable mirror technologies for astronomy at CILAS. Proc. of SPIE Vol. 7015, 70150O (2008),
[7] Leckie, B.; Gardhouse, W.; Fletcher; M. Wooff and Hardy, R. T.. FLAMINGOS-2 OIWFS, Proc. of SPIE Vol. 6269, 626945 (2006)
[8] Baranec, C.; High-order wavefront sensing system for PALM-3000, Proc. of SPIE Vol. 7015, 70155M (2008)
[9] Lai, O.; Chun, M.; Cuillandre, J. C. R.; et al. `IMAKA: Imaging from Mauna KeA with an atmosphere corrected 1 square degree optical imager. Proc. of SPIE Vol. 7015, 70154H (2008)